Available online at www.sciencedirect.com

ScienceDirect

Bioorganic & Medicinal Chemistry 16 (2008) 34–39

Bioorganic & Medicinal Chemistry

Inducing the replacement of PNA in DNA·PNA duplexes by DNA

Tom N. Grossmann,[a] Shunta Sasaki,[a,b] Markus Ritzefeld,[a]
Sung Won Choi,[c] Atsushi Maruyama[c] and Oliver Seitz[a,*]

[a]*Institut für Chemie, Humboldt-Universität zu Berlin, Brook-Taylor-Str. 2, D-12489 Berlin, Germany*
[b]*Department of Chemistry, Graduate School of Science, Kyoto University, Kitashirakawa Oiwakecho, Sakyo-ku, Kyoto 606-8501, Japan*
[c]*Institute for Materials Chemistry and Engineering, Kyushu University, Hakozaki, Higashi-ku, Fukuoka 812-8581, Japan*

Received 21 December 2006; revised 5 April 2007; accepted 27 April 2007
Available online 6 May 2007

Abstract—The uncharged DNA-analogue peptide nucleic acid (PNA) can invade into dsDNA by displacing the non-complementary DNA strand. The formed strand displacement complexes can create a sterical hindrance to block access of enzymes such as nucleases and polymerases. Due to the high stability of DNA·PNA duplexes it is usually not possible to displace the PNA strand by ssDNA or ssRNA. We herein report that the polycationic, comb-type copolymer αPLL-*g*-Dex can induce such a replacement of PNA in DNA·PNA duplexes by ssDNA. The influence of the copolymer on strand exchange highly depends on the nature of the oligonucleotides. Acceleration has only been observed when both the starting duplex and the single-stranded exchanger strand were negatively charged. The presented approach should allow the withdrawal of PNA induced sterical hindrance of DNA by rehybridisation with ssDNA.

1. Introduction

Strand exchange between double-stranded (ds) and single-stranded (ss) oligonucleotides is a key process in living systems and in a multitude of DNA-targeted technologies. In nature, strand exchanges are basic steps in genetic recombination and repair of DNA damage. Probe technologies involved in genotyping[1] and DNA medicines[2] rely on an effective and selective targeting of a particular DNA or RNA sequence. In this context the use of artificial DNA-analogues with optimized DNA-binding properties has been studied. For example, peptide nucleic acids (PNA), bearing an uncharged *N*-(2-aminoethyl)glycine backbone, exhibit a high chemical and biological stability, and bind to complementary DNA or RNA with affinities significantly higher than those of the corresponding DNA.[3] PNA has been used in the development of innovative probe technologies and as a new option to modify or knock-out gene function.[4] One of the intriguing opportunities offered by PNA is invasion into dsDNA by displacing the non-complementary DNA strand.[5] PNA hybridisation can create a sterical hindrance to block access of enzymes such as nucleases and polymerases.[6] Due to the high stability of DNA·PNA duplexes it is not possible to displace the PNA strand by ssDNA or ssRNA. We considered it worthwhile to seek for methods that allow displacement of PNA in a DNA·PNA complex and suppose that the feasibility of removing the PNA-mediated blockage of enzymatic action on DNA would offer interesting opportunities in molecular biology.

A very effective way to modulate DNA strand exchange reactions is provided by the use of polycationic comb-type copolymers, such as αPLL-*g*-Dex (**1**), composed of a cationic poly(L-lysine) backbone and water-soluble side chains of dextran.[7] Copolymer **1** increases the stability of DNA duplexes and triplexes by reducing the counterion condensation during duplex or triplex formation.[8] In addition, polycation **1** affects the kinetics of strand exchange reactions. Notably, copolymer **1** was found to accelerate DNA strand exchange reactions between dsDNA and its homologous single strand at a much faster rate (300- to 1500-fold) than spermine and cethyl trimethyl ammonium bromide.[9] It has been assumed that the copolymer reduces the activation energy of strand exchange reactions by stabilizing the

---

Keywords: Strand exchange; Peptide nucleic acid (PNA); Comb-type copolymer; DNA; Hybridization; FRET; Cationic block-copolymer; Kinetics.

* Corresponding author. E-mail: oliver.seitz@chemie.hu-berlin.de

0968-0896/$ - see front matter © 2007 Elsevier Ltd. All rights reserved.
doi:10.1016/j.bmc.2007.04.066

nucleation complex formed between a parent dsDNA and the ssDNA.[9b]

In this report, we present that the use of copolymer **1** allows the modulation of strand exchange reactions that involve uncharged PNA strands. To monitor strand exchange reactions a fluorescence-based readout system was developed. It is shown that the replacement of the PNA strand in DNA·PNA duplexes by ssDNA is feasible. This study not only presents a possible method for removing PNA-mediated blockage of DNA function but also provides further insights into the mechanism and driving forces of polymer mediated strand exchanges in general.

2. Results and discussion

To investigate strand exchange reactions in real time we used a fluorescence-based readout system (Fig. 1).[9b,10] Target strand **T** is designed to be complementary to the exchange strands (**E**, **E***). The starting oligonucleotide duplex (**T**·**E***) is equipped with a fluorescence donor(F)/acceptor(Q) pair. Fluorescence of donor labelled oligonucleotide **E*** is quenched prior to strand exchange, due to close proximity to the acceptor. Upon strand exchange fluorophore labelled **E*** is replaced by a non-labelled oligonucleotide of the same sequence (**E**) resulting in an increase of donor fluorescence. This setup allows specific detection of strand displacement. The structure of αPLL-*g*-Dex (**1**) and the sequences of the used DNA target (**T**), DNA (**E**, **E***) and PNA (**X**, **X***) exchange strands are shown in Figure 2. αPLL-*g*-Dex (**1**) was synthesized and characterized following reported procedures.[7] **E*** and **X*** bear 6-carboxyfluorescein (FAM) as fluorescence donor and **T** bears 4-[4-(dimethylamino)phenylazo]benzoyl (Dabcyl) as quencher.

The practicability of this setup was tested by investigating the influence of αPLL-*g*-Dex (**1**) on the strand exchange of dsDNA with ssDNA (**T**·**E*** + **E** → **T**·**E** + **E***, Fig. 1). Figure 3a shows the time dependent intensity of FAM fluorescence in absence (solid line) and presence (dashed line) of copolymer **1**. At the beginning single-stranded **E*** was the only oligonucleotide in solution. Upon addition of 1 equiv **T** a decrease in the fluorescence intensity was observed due to the formation of duplex **T**·**E***. The addition of copolymer **1** (dashed line) resulted in a further reduction of the fluorescence intensity probably caused by duplex stabilization (see below)

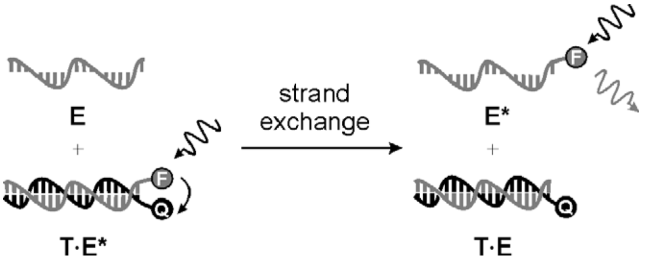

Figure 1. Strand exchange of a FAM labelled DNA strand (**E***) by a non-labelled DNA strand of the same sequence (**E**).

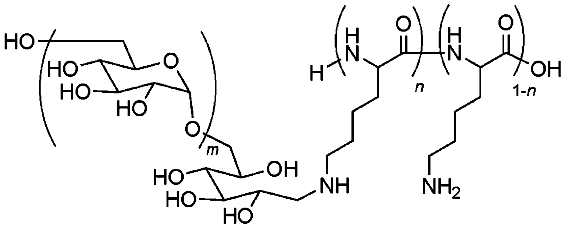

αPLL-g-Dex (1)

DNA target strand

T	$^{3'}$Dabcyl–AAG GGG TGT GGT TGT C$^{5'}$

DNA exchange strands

E	$^{5'}$TTC CCC ACA CCT ACA G$^{3'}$
E*	FAM–$^{5'}$TTC CCC ACA CCT ACA G$^{3'}$

PNA exchange strands

X	Ac-HN ttc ccc aca cct aca g Gly Gly CONH$_2$
X*	FAM–ttc ccc aca cct aca g Gly Gly CONH$_2$

Figure 2. Structure of αPLL-*g*-Dex (**1**) and sequences of used DNA (**T**, **E**, **E***) and PNA (**X**, **X***) single strands.

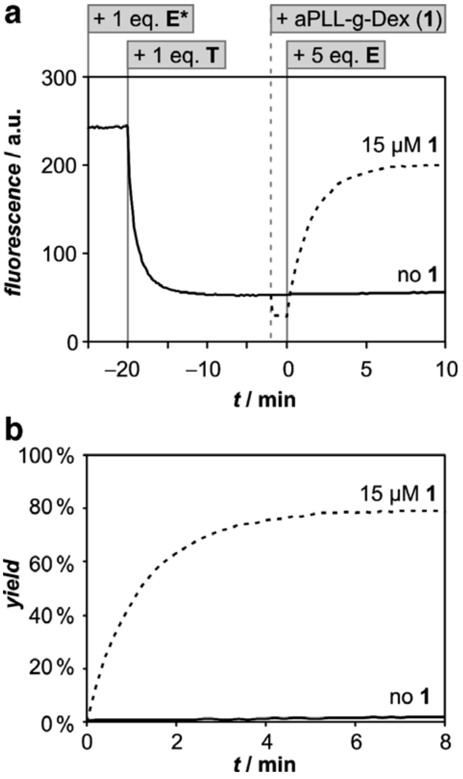

Figure 3. Time courses of **T**·**E*** + **E** → **T**·**E** + **E*** in absence (solid line) and presence (dashed line) of copolymer **1** (15 µM cation concentration, **1**/**T** charge ratio = 5) (a) FAM fluorescence; (b) exchange yield (fluorescence intensity of free **E*** was set 100% and fluorescence at $t = 0$ was set 0% yield). (Spectrometer settings: λ-ex = 485 nm (slit 5 nm), λ-em = 525 nm (slit 10 nm); probes: 0.2 µM **T**, 0.2 µM **E***, 1 µM **E**; buffer: 10 mM NaH_2PO_4, 10 mM NaCl, pH 7; $T = 20$ °C).

bringing the donor/acceptor pair in closer proximity. In absence of copolymer **1** the addition of 5 equiv non-labelled DNA **E** had almost no influence on the fluorescence intensity. Whereas in presence of 15 µM copolymer **1** a rapid increase in fluorescence intensity was observed, caused by a fast displacement of **E*** by the non-labelled oligonucleotide **E**.

Figure 3b shows the time courses of the exchange yield in absence (solid line) and presence (dashed line) of copolymer **1**. In absence of copolymer **1** the strand exchange proceeded slowly providing 1% yield after 6 min. Within the same time in presence of **1** we observed 79% exchange yield. The rate acceleration based on the ratio of the initial exchange rates is 418 which is consistent with values observed for other sequences.[9] Due to 5-fold excess of **E** compared to **E*** a maximal exchange yield of 83% is expected when assuming the same duplex stability for **T·E** and **T·E***. The observed maximum of 79% is in good agreement with this estimation.

The stability of involved oligonucleotide duplexes has an important impact on the thermodynamics of the strand exchange. To minimize the influence of the labels on the exchange reaction the duplex stability should be insensitive to the presence of the Dabcyl and FAM label. Therefore, melting temperatures of the DNA·DNA (**T·E**, **T·E***) and DNA·PNA (**T·X**, **T·X***) duplexes were determined (Fig. 4). In absence of copolymer **1** (dark grey bars) the monolabeled and bislabeled DNA·DNA (**T·E**, **T·E***) and DNA·PNA (**T·X**, **T·X***) duplexes, respectively, exhibit a similar stability. As expected DNA·DNA duplexes are less stable than their DNA·PNA analogues. In presence of copolymer **1** (light grey bars) all duplexes exhibit a similar stability. The observed increase in DNA·DNA duplex stability of ca. 20 °C is consistent with reported observations.[9] The influence of copolymer **1** on the stability of DNA·PNA complexes is negligible due to the lack of the counterion condensation upon duplex formation of uncharged PNA with DNA.[11]

We investigated exchange reactions on the DNA scaffold (**T**) at 30 °C (Fig. 5) using several combinations of DNA and PNA as parent duplex forming strand (**E***, **X***) and exchange strand (**E**, **X**). The temperature was chosen as it allowed the observation of most exchange reactions in reasonable periods of time. The exchange reactions are ordered by the value of their initial rate in absence of copolymer **1** (dark grey bars). Under these conditions displacement of PNA in a DNA·PNA duplex by ssDNA (**T·X*** + **E**) is the slowest reaction with a not detectable exchange rate. The displacement of PNA by ssPNA (**T·X*** + **X**) proceeds faster but still 22 times slower than the ‘natural’ exchange reaction of dsDNA with ssDNA (**T·E*** + **E**). The fastest exchange in absence of copolymer **1** is the strand displacement of DNA by ssPNA (**T·E*** + **X**). This is the pseudo reverse reaction of the slowest strand exchange (**T·X*** + **E**) and known to proceed very quickly.[5]

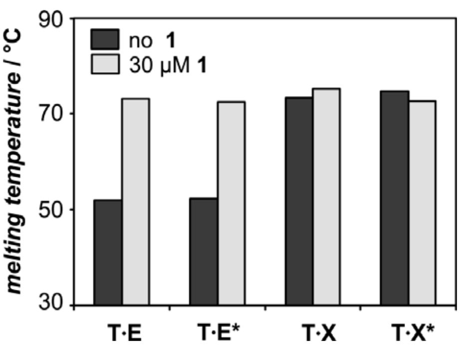

Figure 4. Melting temperatures of DNA and PNA oligonucleotides with target DNA **T** in absence (dark grey bars) and presence (light grey bars) of copolymer **1** (30 µM cation concentration, **1/T** charge ratio = 2). For values, see Section 4.

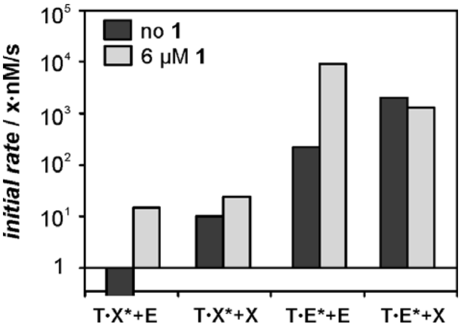

Figure 5. Initial strand exchange rates in absence (dark grey bars) and presence (light grey bars) of copolymer **1** (6 µM cation concentration, **1/T** charge ratio = 2) at 30 °C. Initial rates [nM/s] were multiplied by $x = 2.08 \times 10^4$ setting the value for **T·X*** + **X** in the absence of **1** to 10. For values, see Section 4.

It can be concluded that the displacement of PNA strands (**T·X*** + **E** and +**X**) proceeds significantly slower than the displacement of DNA strands (**T·E*** + **E** and +**X**), which can be explained with the higher DNA·PNA duplex stability and, therefore, presumably higher activation barrier. The comparison of **T·X*** + **E** with **T·X*** + **X**, and of **T·E*** + **E** with **T·E*** + **X**, reveals that ssPNA (**X**) exhibits a higher capability to enforce strand displacement than ssDNA (**E**). In the presence of 6 µM copolymer **1** (Fig. 5, light grey bars) we observed the expected increase in the initial rate of the ‘natural’ all DNA system (**T·E*** + **E**). Remarkably, copolymer **1** proved able to induce the displacement of PNA by ssDNA (**T·X*** + **E**), resulting in an initial rate higher than the one of PNA-to-PNA exchange (**T·X*** + **X**) in absence of copolymer **1**.

Rather than comparing the initial rates in the logarithmic scale of Figure 5 it is instructive to discuss the ratio of the initial rates in presence and absence of copolymer **1** (rate acceleration) in Figure 6a. Upon addition of copolymer **1** PNA strand displacement by ssDNA (**T·X*** + **E**) exhibits a considerable rate acceleration (>140), whereas the PNA strand displacement by ssPNA (**T·X*** + **X**) shows only a small increase in the exchange rate (2.4-fold). A rate acceleration of 39.6 for the all DNA system (**T·E*** + **E**) at a charge ratio **1/T** = 2 is in line with reported observations.[9] However, for the DNA strand displacement by ssPNA (**T·E*** + **X**) we observed an almost negligible decrease of factor 1.6.

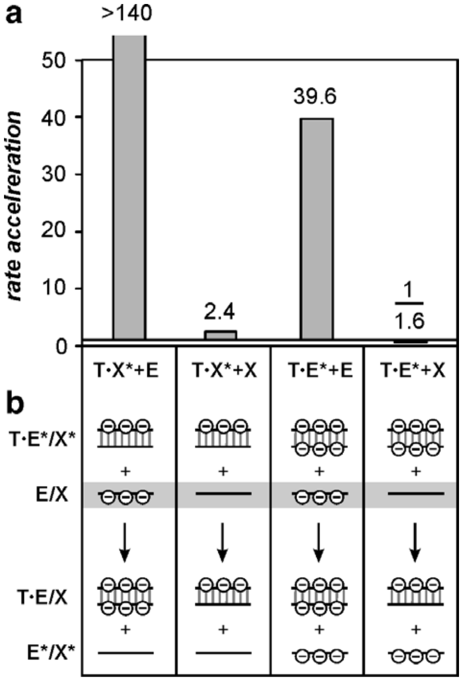

Figure 6. (a) Rate acceleration (ratio of initial rate in presence/absence of **1**) upon addition of **1** (6 μM cation concentration, **1**/**T** charge ratio = 2) at 30 °C; (b) schematic overview of types of backbones involved in strand exchange.

To explain these observations one could consider a model, in which the cationic copolymer **1** acts by binding several negatively charged oligonucleotides. This may result in an increase of the effective molarity and may support the formation of nucleation complexes between a partially unwound parent duplex and its homologous single strand.[9b,12] According to this consideration, the copolymer-induced acceleration of strand exchange rates can only be achieved when both the starting double strand and the single strand exchanger are negatively charged (Fig. 6b). As the DNA target **T** is part of all occurring duplexes and renders these negatively charged, the nature of the starting single strand (**E** or **X**) is of central importance for the effectiveness of the copolymer (grey bar in Fig. 6b). Therefore, only exchange reactions with starting ssDNA **E** (**T**·**E*** + **E** and **T**·**X*** + **E**) undergo accelerated strand displacement, whereas reactions with the uncharged ssPNA **X** (**T**·**E*** + **X** and **T**·**X*** + **X**) experience a negligible influence of copolymer **1** on the reaction rate. The enormous acceleration of PNA displacement by ssDNA (**T**·**X*** + **E** → **T**·**E** + **X***) is additionally supported by the lack of coulomb attraction between the exchanged PNA strand **X*** and the cationic copolymer **1**. Therefore, PNA strand **X*** is released from the copolymer, disfavouring the reverse reaction. In conclusion, cationic copolymer **1** can induce increases in the exchange rate of DNA·DNA and DNA·PNA duplexes by ssDNA but not by ssPNA.

3. Conclusions

We have performed real time measurements of strand exchange reactions on a DNA template with participation of DNA and PNA exchange strands. In particular, we were interested in the influence of αPLL-*g*-Dex (**1**) on strand exchange reactions. Copolymer **1** was found to accelerate exchange reactions when both starting oligonucleotides, single and double strand, were negatively charged. In this context, it was sufficient to apply parent double strands formed by an uncharged PNA and a negatively charged DNA strand but necessary to use ssDNA as exchanging strand. Therefore, in presence of copolymer **1** we observed displacement of PNA strands in DNA·PNA duplexes by analogous ssDNA, not observed in absence of copolymer **1**. To our best knowledge this is the first time a strand displacement of PNA by analogous ssDNA has been reported. This approach allows in principle the withdrawal of PNA induced sterical hindrance of DNA by rehybridisation with ssDNA. This reversible hindrance of DNA should allow the development of switchable blockages of enzymatic action on DNA.

4. Experimental

4.1. Materials and instruments

PNA monomers were purchased from Applied Biosystems. PyBOP, HCTU, Novagen TGR resin and Fmoc-Gly-OH were purchased from Novabiochem. DNA was purchased from BioTeZ Berlin-Buch GmbH, Germany, in HPLC quality. 6-Carboxyfluorescein (FAM–OH) and dry DMF (H_2O < 0.01%) were purchased from Fluka. αPLL-*g*-Dex was synthesized following reported procedures.[7] Water was purified with a Milli-Q ultra pure water purification system. Automated linear solid-phase synthesis was performed by using an Intavis ResPep parallel synthesizer equipped with microscale columns for PNA synthesis. Analytical HPLC was performed with a Merck–Hitachi Elite LaChrom chromatograph (column: Varian Polaris C18 Å 5 μm 250 × 46, pore size 220 Å) at 55 °C. Semipreparative HPLC was performed on an Agilent 1100 series instrument (column: Varian Polaris C18 Å 5 μm 250 × 100, pore size 220 Å). Eluents: A (98.9% H_2O, 1% acetonitrile, 0.1% TFA) and B (98.9% acetonitrile, 1% H_2O, 0.1% TFA) were used in a linear gradient with a flow rate of 1 mL/min for analytical and 6 mL/min for semipreparative HPLC. MALDI-TOF mass spectra were recorded with a Voyager-DE Pro Biospectrometry workstation of PerSeptive Biosystems (matrix: sinapinic acid). UV spectra were recorded using a Varian Cary 100 spectrometer (UV quartz cuvettes: 4 × 10 mm). Fluorescence spectra were recorded using a Varian Cary Eclipse spectrometer (fluorescence quartz cuvettes: 4 × 10 mm).

4.2. Loading of Novagen TGR resin

The resin (250 mg, 0.29 μmol/g) was allowed to swell in 10 mL DMF (10 mL, 30 min). For Fmoc-removal the resin was twice treated with DMF/piperidine (4:1, 1.5 mL) and subsequently washed (5× DMF, 5× CH_2Cl_2, 5× DMF). For preactivation PyBOP (250 μmol) and NMM (375 μmol) were added to a solution of Fmoc-protected glycine (250 μmol) in

DMF (1.5 mL). After 3 min, the mixture was added to the resin (2.5 h) and washed (5× DMF, 5× CH_2Cl_2, 5× DMF). For capping, the resin was treated with a solution of Ac_2O/pyridine (1:9, 5 min, 1.5 mL). The resin was washed (5× DMF, 5× CH_2Cl_2) and finally dried under reduced pressure.

4.3. Automated solid-phase synthesis according to Fmoc-strategy

Fmoc-cleavage: DMF/piperidine (4:1, 200 µL) was added to the resin. After 2 min, the procedure was repeated once. The resin was washed (7× 200 µL DMF). Coupling: a preactivation vessel was charged with a 0.6 M HCTU solution in DMF (12 µL), a 4 M NMM solution in DMF (4 µL) and a 0.2 M PNA monomer solution in NMP (40 µL). After 8 min, 50 µL of preactivation solution was transferred to the resin. After 30 min, the resin was washed (2× 200 µL DMF). Capping: Ac_2O/2,6-lutidine/DMF (5:6:89, 200 µL) was added. After 3 min the resin was washed (2× DMF).

4.4. Cleavage and purification of PNA-probes

A solution of cysteine methyl ester hydrochloride (3 mg) in TFA/*m*-cresol/H_2O (18:1:1, 600 µL) was added to the resin. After 30 min the resin was washed with TFA (4× 200 µL). For purification the combined filtrates were concentrated under reduced pressure before addition of diethyl ether. The precipitated crude product was dissolved in water and purified by semipreparative HPLC. After the eluent was removed under reduced pressure, the product was dissolved in H_2O.

4.5. Determination of yields

An aliquot was diluted with buffer (10 mM NaH_2PO_4, 10 mM NaCl, pH 7) to 1 mL and the optical density measured at 260 nm by using a quartz cuvette with a 1 cm path length. The sample concentration was calculated by using oligo calculation at www.gensetoligos.com.

4.6. $^{\text{Ac–HN}}$ttc ccc aca cct aca g Gly Gly$^{\text{CONH}_2}$ (X)

The PNA sequence was assembled via automated solid-phase synthesis in 2 µmol scale on an Fmoc-Gly-Novagen TGR resin (11.1 mg, 0.180 mmol/g). The resin was then treated with DMF/piperidine (4:1, 2× 5 min, 0.5 mL) and washed (5× DMF, 5× CH_2Cl_2, 5× DMF). The addition of pyridine/Ac_2O (10:1, 5 min, 1 mL) was followed by washing (5× DMF, 10× CH_2Cl_2). Cleavage and purification steps followed as reported before. $OD_{260} = 51.5$ (353 nmol, 18%). HPLC: $t_R = 15.6$ (3% A—30% A in 30 min). MALDI-TOF-MS: m/z = 4375.8 ($[M+H]^+$, calculated 3475.2). $C_{174}H_{222}N_{90}O_{50}$ (MW = 4374.20).

4.7. FAM—ttc ccc aca cct aca g Gly Gly$^{\text{CONH}_2}$ (X*)

The PNA sequence was assembled via automated solid-phase synthesis in 2 µmol scale on an Fmoc-Gly-Novagen TGR resin (11.1 mg, 0.180 mmol/g). After treatment with DMF/piperidine (4:1, 2× 5 min, 0.5 mL) the resin was washed (5× DMF, 5× CH_2Cl_2, 5× DMF). FAM–OH (10 µmol), PyBOP (10 µmol) and NMM (20 µmol) in DMF (400 µL) were added (2× 1 h) and the resin was finally washed (5× DMF, 5× CH_2Cl_2, 5× DMF). The addition of pyridine/Ac_2O (10:1, 5 min, 1 mL) was followed by treatment with DMF/piperidine (4:1, 5 min, 1 mL) and washing (5× DMF, 10× CH_2Cl_2). Cleavage and purification steps followed as reported before. $OD_{260} = 34.0$ (218 nmol, 11%). HPLC: $t_R = 14.5$ (3% A—60% A in 30 min). MALDI-TOF-MS: m/z = 4691.1 ($[M+H]^+$, calculated 4691.5). $C_{193}H_{230}N_{90}O_{55}$ (MW = 4690.46).

4.8. Melting temperature (T_M) measurements

UV melting curves were measured at 260 nm by using a Varian Cary 100 spectrometer equipped with a peltier block. A degassed aqueous solution (10 mM NaH_2PO_4, 10 mM NaCl, pH 7) was used as buffer. The oligonucleotides were mixed at 1:1 stoichiometry, and the solutions were adjusted to a final duplex concentration of 1 µM. Prior to analysis, the samples were heated to the maximum temperature of 85 °C and cooled to starting temperature of 20 °C. Melting curves were recorded at a rate of 0.5 °C/min. T_M values were defined as the maximum of the first derivative of the melting curve. The following table shows the T_M values presented in Figure 4.

T_M/°C	**T·E**	**T·E***	**T·X**	**T·X***
no **1**	51.8	52.2	73.3	74.7
30 µM **1**	73.1	72.4	75.1	72.5

4.9. Measurement of initial rates of strand exchange

Measurements were carried out in a buffered solution (10 mM NaH_2PO_4, 10 mM NaCl, pH 7). Time courses of FAM fluorescence were measured using the following settings: λ-ex = 485 nm (slit 5 nm), λ-em = 525 nm (slit 10 nm). **T**, **E**, **E***, **X** and **X*** were diluted in H_2O (ca. 100 µM) to serve as stock solutions. To the buffer (final volume 1 mL) the appropriate amount of **E*** or **X*** (0.2 nmol, 1 equiv) was added followed by the addition of **T** (0.2 nmol, 1 equiv). If required copolymer **1** (6 nmol cations, **1/T** charge ratio = 2) was added. After fluorescence intensity reached its minimum **E** or **X** (1 nmol, 5 equiv) was added. The following table shows the initial rates presented in Figure 5. There was no strand displacement detectable for the reaction **T·X* + E** in absence of **1**. The value of 5×10^{-6} nM s^{-1} is a conservative estimation for the minimal initial rate that can be detected under these conditions.

Initial rate/nM s^{-1}	**T·X* + E**	**T·X* + X**	**T·E* + E**	**T·E* + X**
no **1**	$<5 \times 10^{-6}$	4.8×10^{-4}	1.1×10^{-2}	9.7×10^{-2}
6 µM **1**	7.2×10^{-4}	1.2×10^{-3}	4.2×10^{-1}	6.1×10^{-2}

Acknowledgments

T.N.G. is grateful for a fellowship from the Studienstiftung des deutschen Volkes. S.W.C. was supported by a Japan Society for the Promotion of Science (JSPS) postdoctoral fellowship.

References and notes

1. Selected reviews: (a) Kricka, L. J. *Ann. Clin. Biochem.* **2002**, *39*, 114–129; (b) Strerath, M.; Marx, A. *Angew. Chem. Int. Ed.* **2005**, *44*, 7834–7849; (c) Kwok, P. Y. *Annu. Rev. Genomics Hum. Genet.* **2001**, *2*, 235–258.
2. Selected reviews: (a) Hannon, G. J. *Nature* **2002**, *418*, 244–251; (b) Uhlmann, E.; Peyman, A. *Chem. Rev.* **1990**, *90*, 543–584; (c) Opalinska, J. B.; Gewritz, A. M. *Nat. Rev. Drug Disc.* **2002**, *1*, 503–514.
3. (a) Nielsen, P.; Egholm, M.; Berg, R.; Buchardt, O. *Science* **1991**, *254*, 1497–1500; Selected review: (b) Uhlmann, E.; Peyman, A.; Breipohl, G.; Will, D. W. *Angew. Chem. Int. Ed.* **1998**, *37*, 2796–2823.
4. (a) Stender, H.; Fiandaca, M.; Hyldig-Nielsen, J. J.; Coull, J. *J. Microbiol. Methods* **2002**, *48*, 1–17; (b) Brandt, O.; Hoheisel, J. D. *Trends Biotechnol.* **2004**, *22*, 617–622; (c) Dose, C.; Ficht, S.; Seitz, O. *Angew. Chem. Int. Ed.* **2006**, *45*, 5369–5373; (d) Grossmann, T. N.; Seitz, O. *J. Am. Chem. Soc.* **2006**, *128*, 15596–15597; (e) Ficht, S.; Mattes, A.; Seitz, O. *J. Am. Chem. Soc.* **2004**, *126*, 9970–9981; (f) Köhler, O.; Jarikote, D. V.; Seitz, O. *ChemBioChem* **2005**, *6*, 69–77; (g) Janowski, B. A.; Huffman, K. E.; Schwartz, J. C.; Ram, R.; Hardy, D.; Shames, D. S.; Minna, J. D.; Corey, D. R. *Nat. Chem. Biol.* **2005**, *1*, 210–215.
5. (a) Cherny, D. Y.; Belotserkovskii, B. P.; Frank-Kamenetskii, M. D.; Egholm, M.; Buchardt, O.; Berg, R. H.; Nielsen, P. E. *Proc. Natl. Acad. Sci. U.S.A.* **1993**, *90*, 1667–1670; (b) Peffer, N. J.; Hanvey, J. C.; Bisi, J. E.; Thomson, S. H.; Hassman, C. F.; Noble, S. A.; Babiss, L. E. *Proc. Natl. Acad. Sci. U.S.A.* **1993**, *90*, 10648–10652; (c) Smolina, I. V.; Demidov, V. V.; Soldatenkov, V. A.; Chasovskikh, S. G.; Frank-Kamenetskii, M. D. *Nucleic Acids Res.* **2005**, *33*, e146.
6. (a) Komiyama, M.; Ye, S.; Liang, X.; Yamamoto, Y.; Tomita, T.; Zhou, J.-M.; Aburatani, H. *J. Am. Chem. Soc.* **2003**, *125*, 3758–3762; (b) Shakeel, S.; Karim, S.; Ali, A. *J. Chem. Technol. Biotechnol.* **2006**, *81*, 892–899; (c) Belfort, M.; Roberts, R. J. *Nucleic Acids Res.* **1997**, *25*, 3379–3388.
7. (a) Maruyama, A.; Katoh, M.; Ishihara, T.; Akaike, T. *Bioconjugate Chem.* **1997**, *8*, 3–6; (b) Maruyama, A.; Watanabe, H.; Ferdous, A.; Katoh, M.; Ishihara, T.; Akaike, T. *Bioconjugate Chem.* **1998**, *9*, 292–299.
8. (a) Maruyama, A.; Ohnishi, Y.; Watanabe, H.; Torigoe, H.; Ferdous, A.; Akaike, T. *Colloids Surf.* **1999**, *B16*, 273–280; (b) Ferdous, A.; Akaike, T.; Maruyama, A. *Biomacromolecules* **2000**, *1*, 186–193; (c) Ferdous, A.; Akaike, T.; Maruyama, A. *Bioconjugate Chem.* **2000**, *11*, 520–526.
9. (a) Kim, W. J.; Ishihara, T.; Akaike, T.; Maruyama, A. *Chem. Eur. J.* **2001**, *7*, 176–180; (b) Kim, W. J.; Akaike, T.; Maruyama, A. *J. Am. Chem. Soc.* **2002**, *124*, 12676–12677.
10. Bazemore, L. R.; Takahashi, M.; Radding, C. M. *J. Biol. Chem.* **1997**, *272*, 14672–14682.
11. Tomac, S.; Sarkar, M.; Ratilainen, T.; Wittung, P.; Nielsen, P. E.; Norden, B.; Gräslund, A. *J. Am. Chem. Soc.* **1996**, *118*, 5544–5552.
12. Reynaldo, L. P.; Vologodskii, A. V.; Neri, B. P.; Lyamichev, V. I. *J. Mol. Biol.* **2000**, *297*, 511–520.